THE PUBLISHING HOUSE
OF THE ROMANIAN ACADEMY

PROCEEDINGS OF THE ROMANIAN ACADEMY, Series A,
Volume 11, Number 1/2010, pp. 47–54

LOW-FREQUENCY NOISE PREDICTION OF VERTICAL AXIS WIND TURBINES

Horia DUMITRESCU*, Vladimir CARDOŞ*, Alexandru DUMITRACHE*, Florin FRUNZULICĂ*,**

* "Gheoghe Mihoc-Caius Iacob" Institute of Statistics and Applied Mathematics
** "Elie Carafoli" Department of Aerospace Sciences – University "Politehnica" of Bucharest
Corresponding author: E-mail: horiad12@yahoo.com, ffrunzi@yahoo.com

A first study is reported of the influence of unsteady flow on the aerodynamics and aeroacoustics of vertical axis wind turbines by numerical simulation. The combination of aerodynamic predictions with a discrete vortex method and aeroacoustic predictions based on Ffowcs Williams-Hawkings equation is used to achieve this goal. The numerical results show that unsteady flow of the turbine has a significant influence on the turbine aerodynamics and can lead to a decrease in generated noise as compared to the conventional horizontal axis wind turbine at the similar aerodynamic performance.

Key words: Aerodynamics; Unsteady flows; Vortex methods; Dynamic stall; Wind turbines.

1. INTRODUCTION

Rising concern for wind turbine noise as a source of community annoyance has led to the introduction of increasing noise regulations for all wind turbines. In the last time, the problem of wind turbine noise is aggravated by the application of larger machines leading to significant increases in the levels of aerodynamic noise. In the most cases, the major part of the aerodynamic noise of a rotor is generated by blade finite thickness and blade loads accounted for the first and second terms in the Ffowcs Williams-Hawkings equation [1]. The present work addresses the aspect of the radiated low-frequency noise of vertical axis wind turbines. Although the frequency range is below the threshold of human hearing the radiated sound pressure can influence people [2, 3].

2. AERODYNAMIC ANALYSIS

Vortex Model. All calculations of this work were performed with a discrete vortex method [4]. It allows load and flow field calculations of vertical axis wind turbines with straight blades and includes a free wake model. The local air velocity relative to a rotor blade consist of the free-stream velocity, that due to the blade motion and the wake induced velocity (Fig. 1). In order to predict the inflow at the blades it is necessary to describe the blade surfaces and the wake. The blades are simply lifting surfaces of large span, so the each blade of the rotor is represented by a bound vortex lifting line located along the rotor blade quarter chord line with the incident-flow boundary condition met at the three quarter chord location.

The wake consist of shedding spanwise vortex filaments resulted from the temporal variation in loading distributions on the blades as required by Kelvin's theorem. A simple representation of a two-dimensional vortex system associated with a blade element is shown in Fig. 2. The contour encloses both the airfoil and its wake and any change in the bound circulation must be accompanied by an equal and opposite change in circulation in the wake. This model is based on the marching-vortex concept where motion begins from an impulsive start with the subsequent generation of a vortex wake, modeled by a sequence of discrete vortices shed at equal time intervals. Thus, for steady-state motion, the force and moment responses are asymptotically achieved. Vortices which are shed during any given time period can be related to the change in bound vortex with respect to time and position along the blade. All variables associated with a particular point vortex as point coordinates and velocities as well as vortex strengths are identified by a double subscript (i, j). The first subscript denotes the blade element from which the point-vortex originated, while the other subscript denotes the time step at which the vortex originated.

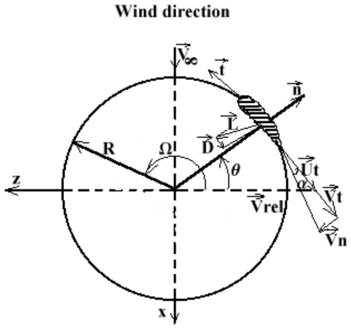

Fig. 1 – Two-dimensional rotor configuration.

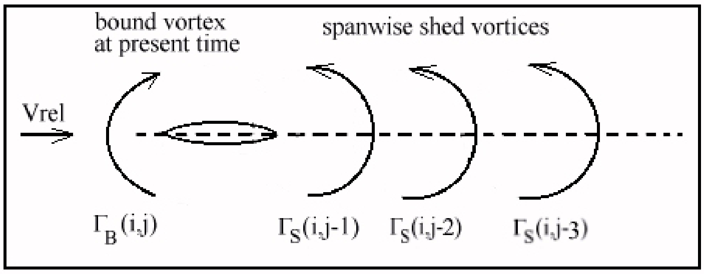

Fig. 2 – Marching-vortex model.

Referring to the diagram of Fig. 2, the spanwise shed vortex strengths can be written as

$$\Gamma_s\left(i, j-1\right) = \Gamma_B\left(i, j-1\right) - \Gamma_B\left(i, j\right). \tag{1}$$

The discrete vortices $\Gamma_S\left(i, j\right)$ are assumed to move downstream with the local fluid velocities given by

$$\mathbf{V}\left(i, j\right) = \mathbf{V}_\infty + \mathbf{V}_I\left(i, j\right), \tag{2}$$

where $\mathbf{V}_\infty$ is the undisturbed freestream velocity and $\mathrm{V}_I\left(i, j\right)$ is the induced velocity by all of discrete vortices in the flow field forming the vortex wake structure. To determine all the point-vortices in the wake, we use

$$\mathbf{r}\left(i, j\right) = \mathbf{r}\left(i, j-1\right) + \mathbf{V}\left(i, j-1\right)\Delta t\,. \tag{3}$$

The induced velocity at the wake points is computed by application of the Biot-Savart law.

Governing Equations. According to the Biot-Savart law, the velocity induced at a point C in a flow by an infinitely long vortex filament of strength Γ is given by

$$\mathrm{V}_I\left(C\right) = \frac{\mathrm{r}\times\Gamma}{2\pi r^2}, \tag{4}$$

where **r** is the position vector from point C to the point vortex. If the point C should happen to come very close to a point vortex, Eq. (4) becomes indeterminate, and a Rankine vortex model (with a viscous core) is used. The vortex core radius r_c can be found assuming that the maximum velocity v_c in the core is equal to the velocity on either side of the vortex sheet springing from the trailing edge of the airfoil

$$v_c = \frac{\Gamma}{2\pi r_c} = \frac{\Gamma}{2R\Delta\theta}\ \left(r_c = \frac{R\Delta\theta}{\pi}\right), \tag{5}$$

where R is the rotor radius and Δθ is azimuthal blade angle step.

The total velocity at a lattice point $\mathbf{V}_I\left(i, j\right)$ is obtained by summing the induced velocities from all other vortices in the flow. With lattice point notation this can be written as

$$\mathbf{V}_I\left(i, j\right) = \sum_{k=1}^{NB}\sum_{l=1}^{NT}\mathbf{V}_{ISV}\left(k, l\right) \tag{6}$$

where $\mathbf{V}_{ISV}$ is the velocity induced by shed vortices, NB is the number of blades and NT is the number of time steps. The closure of the vortex model is the relationship for the bound vortex strength Γ_B which can be related to the local relative air velocity V_{rel}, section chord c and the section lift coefficient $C_L(\alpha)$ through the Kutta-Joukowski law

$$\Gamma_B = \frac{1}{2} C_L c V_{rel} . \tag{7}$$

The local relative velocity in the plane of the airfoil section V_{rel} and local airfoil angle of attack α are functions of the local tangential velocity of the blade element U_T, the induced velocity at the control point on the blade element $\mathbf{V}_I(u,v,w)$, the wind velocity $\mathbf{V}_\infty$ and the azimuthal blade angle θ. Referring to Fig. 1, the following relationships can be obtained

$$\mathbf{V}_{rel} = (V_\infty + u + U_T \cos\theta)\mathbf{i} + (w - U_T \sin\theta)\mathbf{k} , \tag{8}$$

$$V_{rel} = \left[(\mathbf{V}_{rel} \cdot \mathbf{n})^2 + (\mathbf{V}_{rel} \cdot \mathbf{t})^2 \right]^{1/2} , \tag{9}$$

$$\alpha = \tan^{-1} \frac{\mathbf{V}_{rel} \cdot \mathbf{n}}{\mathbf{V}_{rel} \cdot \mathbf{t}} , \tag{10}$$

$$U_T = R\Omega . \tag{11}$$

In the case of low tip-speed ratio (TSR), the vortex methods developed in the past based on the quasi-steady analysis showed large discrepancy due to the effect of dynamic stall on the moving airfoils. A correction based on the Beddoes-Leishman dynamic-stall model [5] was included for unsteady aerodynamics. Thus, the effects of dynamic-stall are now automatically introduced into Eq. (7).

The blade airfoil section tangential and normal-force coefficients C_T and C_N can be written as

$$C_T = C_L \sin\alpha - C_D \cos\alpha, \;\; C_N = -C_L \cos\alpha - C_D \sin\alpha , \tag{12}$$

where the section lift and drag coefficients C_L and C_D are also yielded by the aerodynamic stall model.

The instantaneous blade loadings are defined in terms of the nondimensional normal and tangential forces as follows

$$F_N^+ = \frac{F_N}{1/2\rho c L V_\infty^2} = C_N \left(\frac{V_{rel}}{V_\infty} \right), \tag{13}$$

$$F_T^+ = \frac{F_T}{1/2\rho c L V_\infty^2} = C_T \left(\frac{V_{rel}}{V_\infty} \right), \tag{14}$$

where F_N and F_T are the normal and tangential forces on the blade, ρ is the fluid density; *c* is the airfoil chord length; *L* is the blade length and V_∞ is the freestream velocity.

The average power coefficient for the entire rotor during a single revolution is given by

$$C_P = \frac{\mathrm{TSR}}{\mathrm{NTI}} \frac{c}{2R} \sum_{j=1}^{\mathrm{NTI}} \sum_{i=1}^{\mathrm{NB}} C_{T_{ij}} \left(\frac{V_{rel}}{V_\infty} \right)_{ij}^2 , \tag{15}$$

where *NTI* is the number of the time steps per revolution of the rotor.

Numerical Procedure. For this free wake-lifting line blade method, the unknowns of the problem are both the constant spanwise bound circulation and wake geometry. Since the wake geometry is not a priori known, the numerical procedure requires that calculations be made at successive small time steps until a periodic solution is built up. Initially, there is no wake structure and it is only as the wake develops sufficiently that a periodic solution is obtained. Therefore, the wake geometry is computed employing a time-stepping procedure and the solution for the circulation strength is then obtained at each time step using the above aerodynamic relationships.

The numerical procedure begins with no wake structure and zero bound vortex strength (zero induced velocities). The bound vortex strength and the last value of the induced velocity are then calculated for each blade using Eqs. (7)-(11) and Eq. (6) respectively. The process is repeated until consistent values are obtained for the induced velocities and bound vortices. The computation loop is ended by the calculation of the instantaneous blade forces Eqs. (13), (14) and the new positions of the entire wake point vortices, Eq. (3). Time is increased and a new set of shed vortices is created using Eq. (1). The foregoing procedure may be repeated to obtain the solution at future times. In order to reduce the computational effort the wake is truncated after a periodic solution is achieved (i.e. three rotor revolutions).

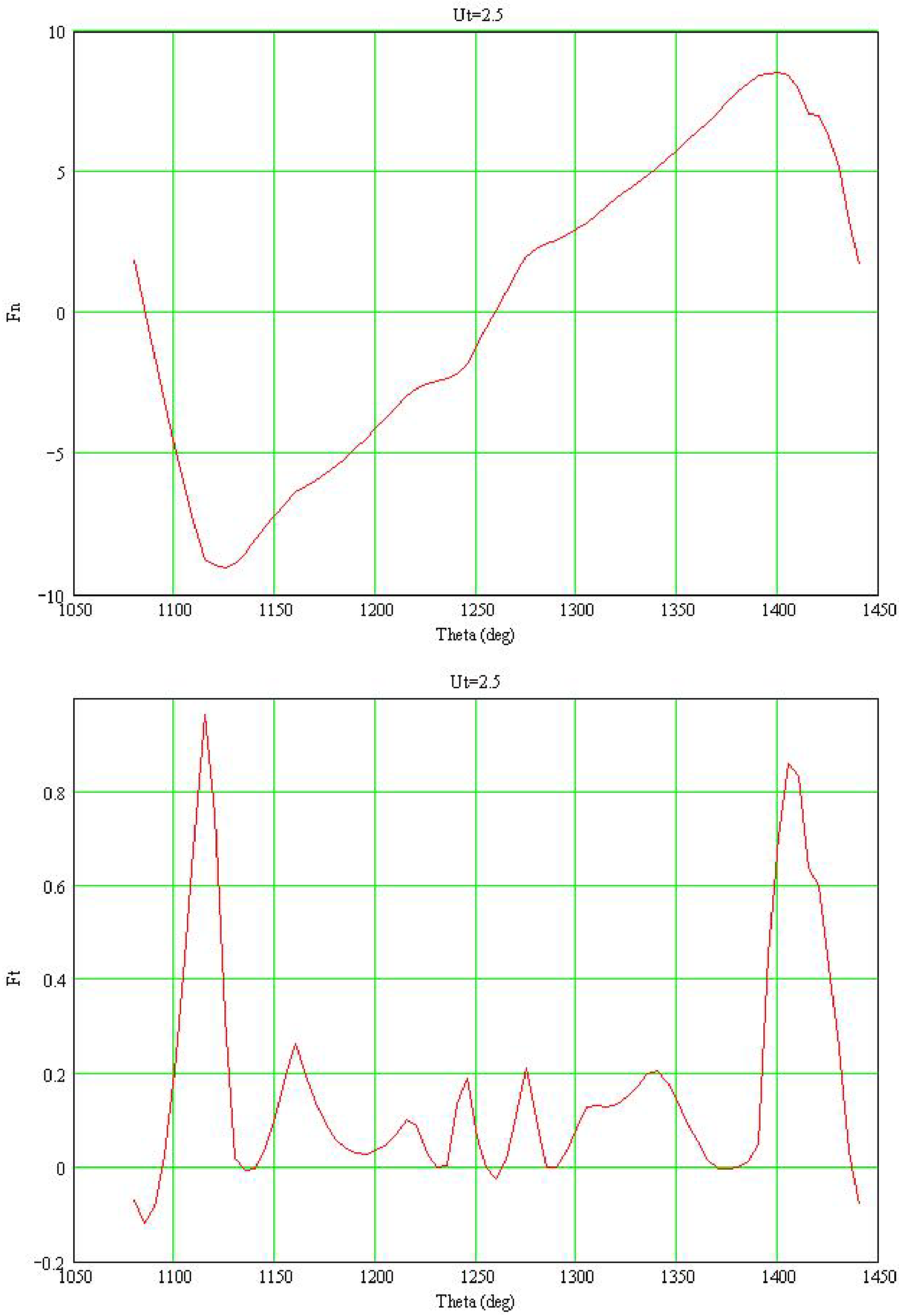

Fig. 3 – Distribution of normal and tangential forces at λ=2.5 .

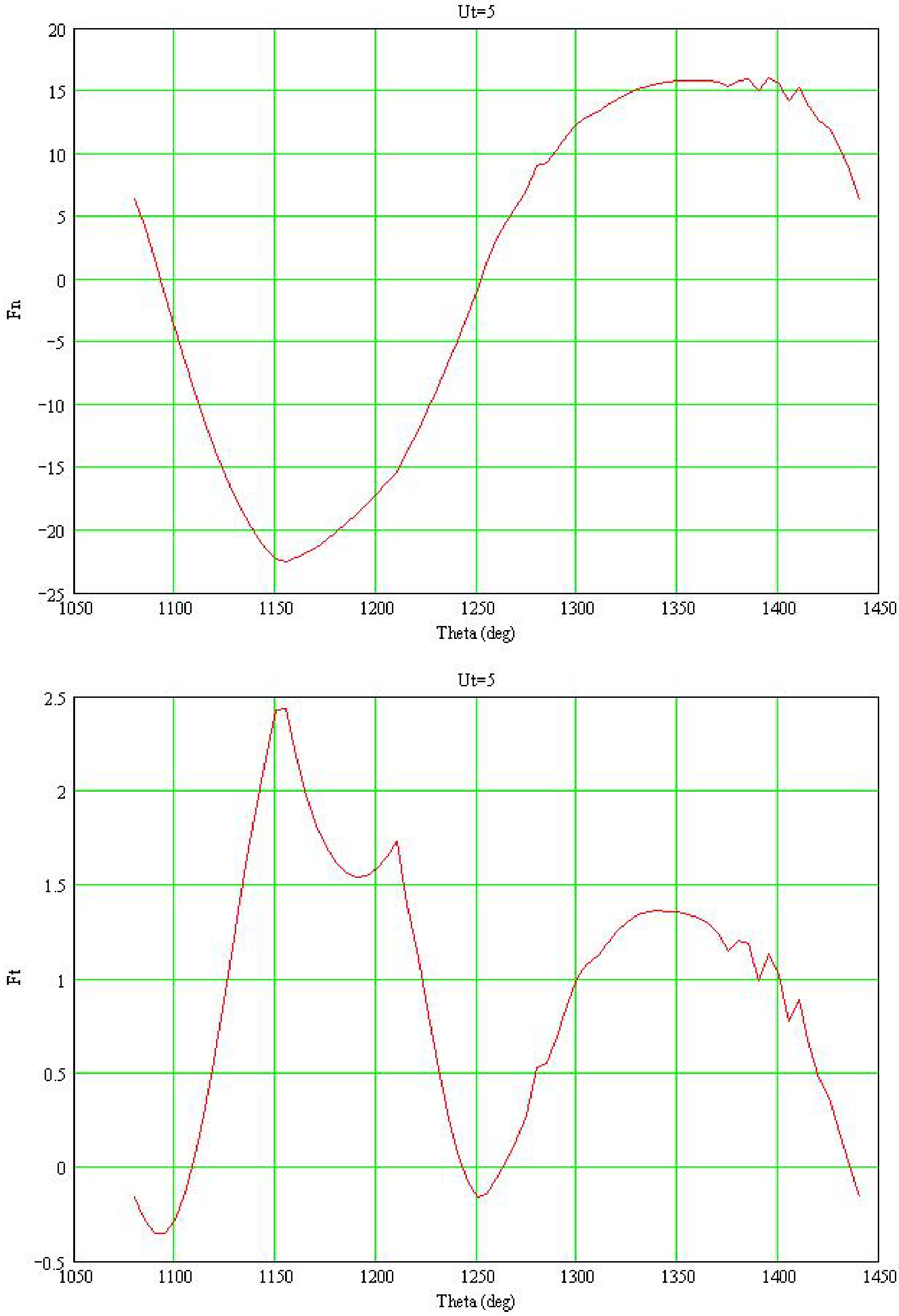

Fig. 4 – Distribution of normal and tangential forces at λ=5.

Numerical Results. Based on the proceeding analysis, a computer program has been developed to predict the force and moments of a vertical axis wind turbine (VAWT). A rotor with two straight blade configuration was designed to operate at an optimum tip speed ratio λ (TSR) of five. An aerodynamic difference between a VAWT and HAWT (horizontal axis wind turbine) is the appearance of unsteady flow phenomena. During a revolution of the rotor of VAWT in a steady wind stream, the flow direction and velocity relative to the rotor blade vary in a cyclic way. The angle of attack becomes about 180 degrees at off design point. This behaviour is stronger at small λ (≤ 3) and the correction of dynamic-stall effects is necessary.

Figures 3 and 4 show the distribution of normal and tangential forces in the case of $\lambda = 2.5$ and 5. It can be seen that at moderate to large λ the downstream ($\theta = 180^0 - 360^0$) blade forces are reduced significantly from those upstream and the positive torque is mainly generated at the upstream.

Figure 5 shows the power coefficient of the VAWT and the conventional HAWT [6]. The maximum power coefficients was the same about 0.40 at λ=5.

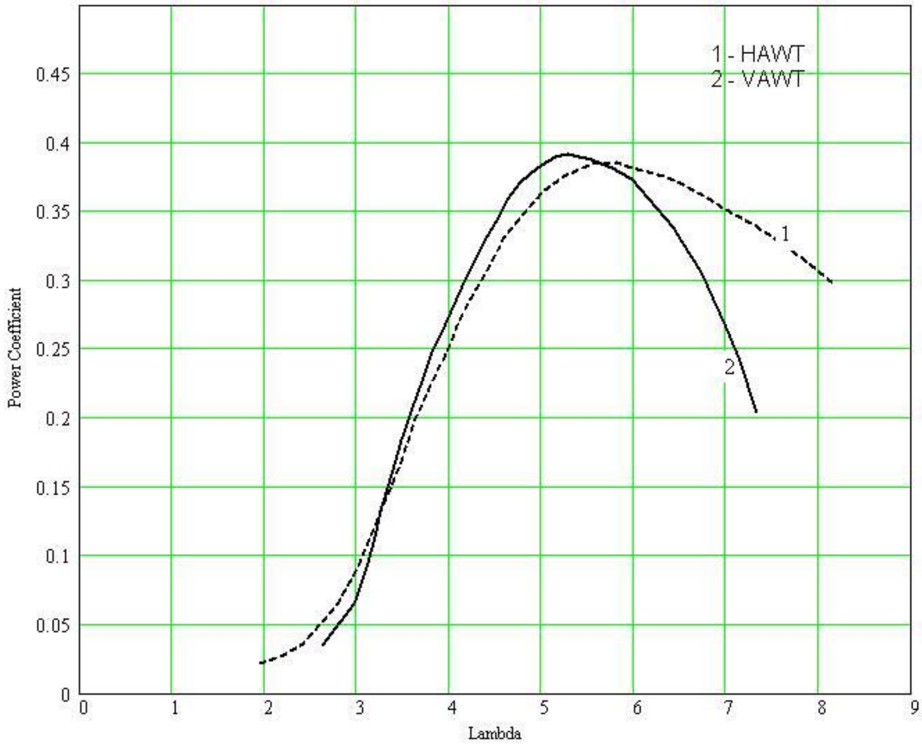

Fig. 5 – Power coefficients.

3. AEROACOUSTIC ANALYSIS

As a next step the aeroacoustics of a two-blade VAWT was calculated using Ffowcs Williams-Hawkings equation [1] and the numerical computation method developed by Succi [7]. The compact body and low Mach number assumptions are used in this computation. Also, this part deals with rotor noise radiating only from blades, thus ignoring the effect of the tower. The simplification provides a better understanding of the basic noise generating mechanisms without additional complexity. The effect of the tower can be introduced later on. Since the relative Mach number is small (0.12), the dipole contribution dominates the aerodynamic noise radiated from low-speed vertical axis wind turbine. Furthermore, the cyclic variation of velocity relative determines effects of the unsteady aerodynamics (intrinsic unsteadiness) besides the unsteadiness due to the motion of sources (dipoles). This unsteady-loading noise dominates the whole aerodynamic radiation and the global noise level is predicted smaller than that of the horizontal axis wind turbine under consideration.

Numerical Results. The acoustic calculation is based on a two-bladed turbine with 10 kW rated power, a rotor diameter of 10 m and a nominal rotational speed of 76 rpm. The noise is estimated at upwind 10 m distance from the rotor axis and the mean wind speed of 8 m/s. Figure 6 shows the computed spectra for the horizontal and vertical rotors with the similar aerodynamic performance. The noise level of the VAWT at λ=5 is about 47 dB, while the value for the HAWT is nearly equal to 56 dB. However, at certain harmonics the sound levels are larger for the vertical rotor. Generally speaking, the non-uniform flow field of a vertical axis wind turbine has a favourable effect on the aerodynamic noise generation.

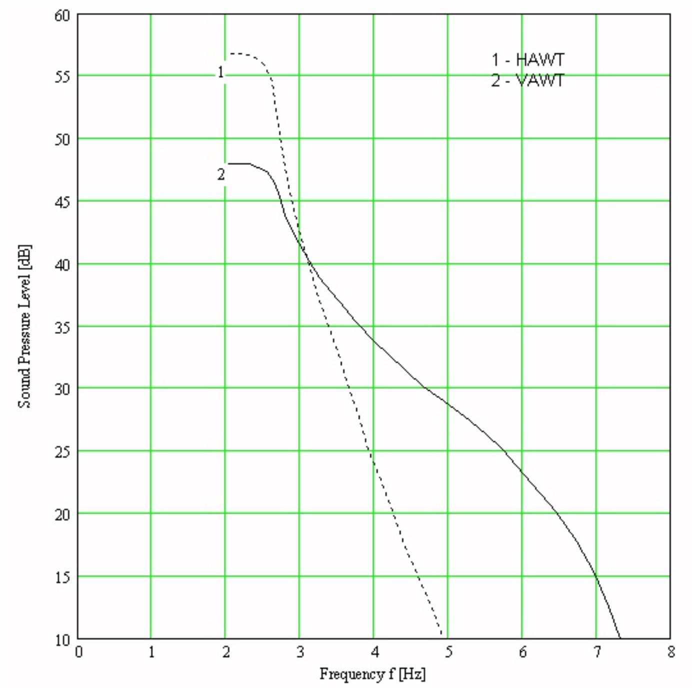

Fig. 6 – Computed spectra for the horizontal and vertical rotors.

4. CONCLUSIONS

The combination of aerodynamic predictions with a discrete vortex model and aeroacoustic predictions based on Ffowcs Williams-Hawkings equation is numerically investigated for a VAWT. The complicated wake structures can be captured with the aerodynamic model and reasonable power coefficient is also obtained. The acoustic analysis shows that the unsteady flow of the VAWT alters the aerodynamic field and can thereby reduce the radiated sound with the increase of its tonal content. The above results indicate that the vertical axis wind turbines are useful options in order to develop the low-noise power generators.

NOMENCLATURE

c	– airfoil chord length
C_D	– drag coefficient
C_L	– lift coefficient
C_M	– moment coefficient
C_N	– normal-force coefficient
C_P	– rotor power coefficient
C_T	– tangential-force coefficient
F_M	– normal force
F_N^+	– dimensionless normal force
F_T	– tangential force
F_T^+	– dimensionless tangential force
i, j	– index
K_I	– empirical constant of dynamic-stall model
$\vec{n}$	– unit vector in normal direction
NB	– number of blades
NT	– number of time steps
NTI	– number of time steps per revolution
$\vec{r}$	– position vector
r_c	– vortex core radius

R – rotor radius
Re – Reynolds number
$\vec{t}$ – unit vector in the chordwise direction
u – induced velocity component in x direction
U_T – rotor tip speed
V_∞, V_w – wind velocity
$\vec{V}_{ISV}$ – velocity vector induced by shed vortices
V_{rel} – relative velocity in plane of airfoil
$\vec{v}$ – induced total velocity vector
w – induced velocity component in z direction
x – wind direction
α – angle of attack
γ – empirical constant
Γ – circulation
Γ_B – bound vortex strength
Γ_S – spanwise vortex strength
θ – Azimuthal blade angle
ρ – fluid density

Subscripts

B – blade
c – core
D – drag
I – induced
L – lift
M – moment
P – power
S – shed

REFERENCES

1. FFOWCS WILLIAMS, J.E., HAWKINGS, D.L., *Sound generation by turbulence and surfaces in arbitrary motion*, Philosophical Transactions on the Royal Society of London, **264**, *A1151*, pp. 321–342, 1969.
2. LOWSON, M.V., *Applications of aeroacoustic analysis to wind turbine noise control*, Journal of Wind Engineering, **16**, *3*, pp. 126–140, 1992.
3. HUBBARD, H.H., SHEPHERD, K.P., *Aeroacoustics of large wind turbines*, Journal of the Acoustical Society of America, **89**, *6*, pp. 2495–2508, 1991.
4. DUMITRESCU, H. CARDOS, V., *A two-dimensional vortex model for vertical axis wind turbines*, Int. J. of Applied Mechanics and Engineering, **7**, *4*, pp.1173–1187, 2002.
5. BEDDOES, T.S., LEISHMAN, J.G., *A semi-empirical model for dynamic stall*, Journal of the American Helicopter Society, **34**, *3*, pp. 3–17, 1989.
6. SCHRECK, S., *The NREL full-scale wind tunnel experiment*, Wind Energy, **5**, pp. 77–84, 2002.
7. SUCCI, G.P., *Design of quiet efficient propellers,* SAE Paper no. 790584, pp. 1–14, 1979.

Received February 28, 2009